ENVIRONMENTAL RESEARCH
LETTERS

LETTER

# The evolution of the geothermal potential of a subsurface urban heat island

**Hannes Hemmerle**[1,*], **Grant Ferguson**[2], **Philipp Blum**[3] **and Peter Bayer**[1]

[1] Department of Applied Geology, Martin Luther University of Halle-Wittenberg, Halle, Germany
[2] Department of Civil, Geological and Environmental Engineering, University of Saskatchewan, Saskatoon, Canada
[3] Institute of Applied Geosciences (AGW), Karlsruhe Institute of Technology (KIT), Karlsruhe, Germany
[*] Author to whom any correspondence should be addressed.

**E-mail:** Hannes.hemmerle@geo.uni-halle.de

**OPEN ACCESS**

**RECEIVED**
25 March 2022

**REVISED**
13 June 2022

**ACCEPTED FOR PUBLICATION**
5 July 2022

**PUBLISHED**
25 July 2022

**Keywords:** shallow geothermal energy, urbanization, groundwater, climate change

Supplementary material for this article is available online

## Abstract

Meeting the rising energy demands of cities is a global challenge. Exploitation of the additional heat in the subsurface associated with the subsurface urban heat island (SUHI) has been proposed to address the heating demands. For the sustainable use of this heat it is crucial to understand how SUHIs evolve. To date, there have been no comprehensive studies showing how temperature anomalies beneath cities change over time scales of decades. Here, we reveal the long-term increase of temperatures in the groundwater beneath Cologne, Germany from 1973 to 2020. The rise in groundwater temperature trails atmospheric temperature rise in the rural areas and exceeds the rise in atmospheric temperature in the urban center. However, the amount of heat that is currently stored each year in the thin shallow aquifer reaches only 1% of the annual heating demand. The majority of the anthropogenic heat passes by the vertical extent of the aquifer or is discharged by the adjacent river. Overall the geothermal resource of the urban ground remains largely underused and heat extraction as well as combined heating and cooling could substantially raise the geothermal potential to supply the city's demand.

## 1. Introduction

Emerging urban expansion and densification cause warming in cities. So-called urban heat islands (UHIs) overprint natural conditions in the atmosphere, at the surface and also in the subsurface [1, 2]. Above ground UHIs have a negative connotation as increased heat stress raises mortality especially during the warm period [3, 4]. Conversely, subsurface UHIs (SUHIs) can have beneficial effects on the shallow geothermal potential of urban aquifers [5, 6]. The rising energy demand for heating and cooling forced by socioeconomic trends and higher cooling loads in response to climate change [7–9] is amplified in cities as the proportion of people who are living in cities is to rise continuously in the 21st century [10, 11].

We are facing this rising energy demand under the necessity to mitigate greenhouse gas emissions and to achieve better integration of renewable energies into our cities [12]. Compared to transmission of electric power, transportation and distribution of thermal energy is not feasible at larger scales [13]. Accessing shallow geothermal energy from urban aquifers yields one of, if not the, most promising alternative to combustion of fossil fuels for thermal applications in cities. Shallow geothermal applications in cities benefit from elevated urban underground temperature in comparison to natural conditions [14, 15]. Given the relatively high energy density of soil and groundwater, this significantly elevates the potential of shallow geothermal systems for heating [5, 6, 16]. Vice versa, elevated temperatures in urban aquifers decrease the potential for space cooling with geothermal energy.

Efficient planning and implementation as well as sustainable operation of shallow geothermal units in urban aquifers require a detailed conceptual knowledge and understanding of the processes that lead to the formation of SUHIs. While above ground the UHI

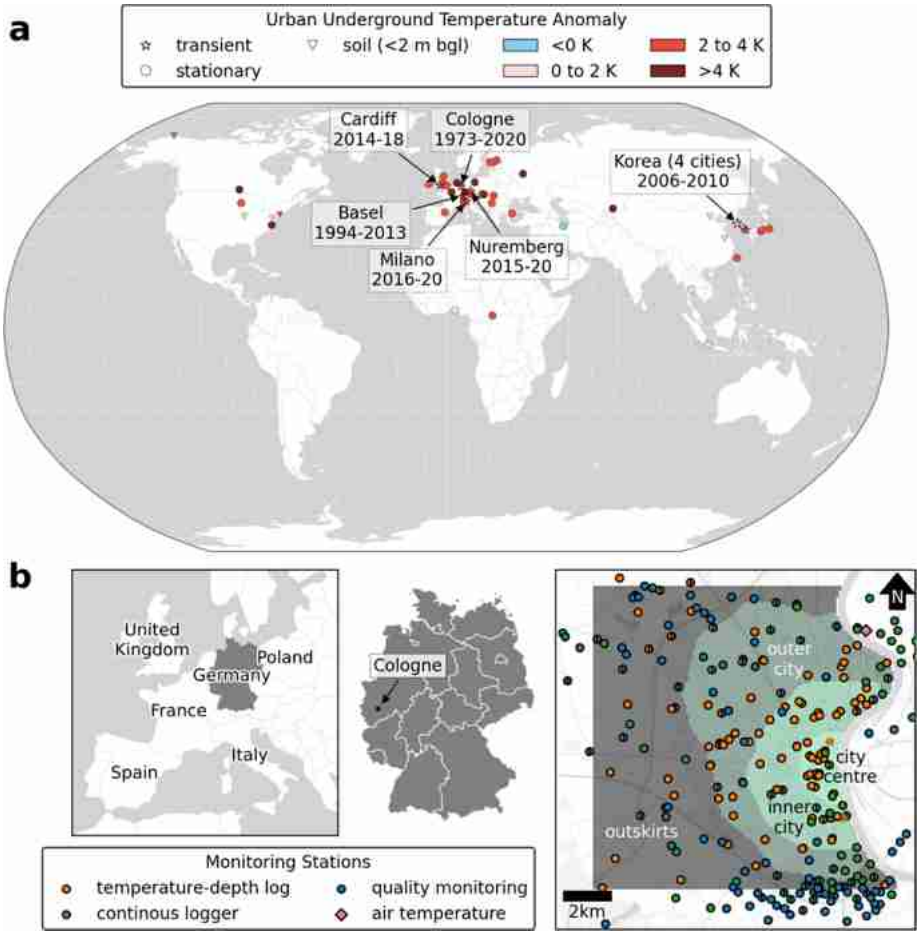


**Figure 1.** (a) Urban underground temperature anomalies. Colors indicate the magnitude of the temperature anomaly in K Markers represent the studied medium. Triangles represent studies in soils at depths shallower than 2 m bgl. Circles and stars are studies in groundwater that either propose stationary temperatures (circles) or transient analysis (stars with labels of city names and studied time periods). (b) Location of temperature monitoring stations in the greater region of Cologne. City zones (city center, inner city, outer city and outskirts) are highlighted for the reference area. Base map accessed from maps.stamen.com (27 May 2021).

phenomenon is well studied and monitored, little so can be said for underground conditions even though SUHI effects have been reported in more than 50 cities globally (figure 1) [2, 16–56]. SUHIs are formed by anthropogenic surface warming that propagates into the subsurface and is enhanced by buried infrastructures, especially if these reach into the water-saturated zone [57–59]. In the subsurface, UHIs typically have average temperature increases between 1 K and 3 K beneath the entire urbanized area, but with pronounced local hot spots. As heat transfer is much slower in the subsurface, short-phased surface variations, such as the seasonal signal, fuse into a year-round stable temperature at depths greater than 10 m below ground level (bgl).

Due to the scarcity in underground temperature monitoring, available studies provide mostly stationary descriptions of the thermal field. Studies that report urban underground temperature over time are extremely rare and typically only comprise few years. Especially in studies covering less than five years, extreme temperature rises that locally exceed $+2$ K dec$^{-1}$ (per decade) are reported [32, 40, 43], while also average temperature rises are above $+0.5$ K dec$^{-1}$ [23, 40, 43]. In many places urban temperature rise more than doubles the expected surface warming in response to climate change [22, 60]. Despite these insights, there is a lack of evidence on how urban underground jointly responds to climate change and anthropogenic warming.

To quantify the geothermal potential of cities, most studies assess the theoretical geothermal potential (TGP) [6], which is the available heat in place for a stationary temperature distribution above natural conditions. The TGP is based on depleting the additional energy in the reservoir and it could be shown that it could in theory supply the annual heating demand in cities for multiple years [5].

The objective of this study is to reveal the long-term evolution of the SUHI phenomena and its significance for future shallow geothermal energy supply in cities. We want to fill this research gap by

presenting unique city-wide subsurface temperature records for the city of Cologne, starting in 1973 [61]. Cologne is one of few cities where extensive groundwater temperature (GWT) monitoring has been performed since the 1970s [61–63] with an urban underground temperature anomaly of up to 4 K reported already in 1974. These early works date back more than three decades before the term SUHI was phrased [2] and are backed up by a variety of recent studies [5, 35, 64–69]. We demonstrate how the thermal field develops and how the urban aquifer is charged by anthropogenic heat emission and climate change. These results offer a unique insight into heat storage rates and SUHI evolution based on data monitored over nearly half a century.

## 2. Materials and methods

### 2.1. Hydrogeology and aquifer structure

The region of interest is located south of the Lower Rhine Basin. The shallow subsurface is composed of Quaternary terrace deposits, that are underlain by Tertiary sediments. The Quaternary deposits host an unconfined aquifer that mainly consists of gravels and sands, while the underlying Tertiary clays, silts, lignite and soft coals down to 200 m bgl function as aquitard [66, 70–72]. The Quaternary-Tertiary boundary (QTB) was used to delineate the bottom of the aquifer. QTB depths are composited from 440 depth values from monitoring wells [73], 97 public borehole profiles [74], and supported by 676 resolved from the isolines of the Quaternary basis map that was kindly provided by the geological survey of North Rhine-Westphalia. Interpolated QTB range between 15 and 81 m asl (above sea level) in the model area. Surface elevation of the public 1 m digital elevation model (DEM) tiles [75] were composited and resampled to 100 m resolution.

### 2.2. Groundwater data

Groundwater data can be classified into three groups: temperature depth logs, temperature and hydraulic head continuous loggers, and temperature recorded during groundwater quality measurements. In total, 266 wells with temperature monitoring were selected for the analysis. *Temperature depth logs* have been performed in 1973 [61], 1977 [62], in 2009 and 2012 [5, 66], and between 2018 and 2020. Temperatures were recorded *in-situ* without pumping as profiles measured from top to bottom. The vertical resolution is increasing towards greater depths and is between 1 and 5 m. Different standard temperature level meters (e.g. SEBA KLL-T) with an accuracy between 0.05 and 0.1 K were used. The drift in absolute temperature between these devices is typically below 0.2 K. For the measurement campaigns in 1973 and 1977 not all recorded profiles were preserved over time. Data from the years 1973 to 1977 are digitized from aquifer temperature maps measured 0.5 m below groundwater level (GWL) in 1973 and in 15 and 20 m bgl in 1977. *Temperature and hydraulic head continuous loggers* are maintained by government institutions (city and district government of Cologne), water suppliers (Rheinenergie AG) and a non-profit public body (Erftverband). Temperature timeseries are available only for 77 stations maintained by the Rheinenergie AG. At these standard groundwater monitoring loggers with temperature accuracy <0.3 K and precision <0.1 K are typically installed less than 5 m bgl. Hydraulic head measurements, both manual and logged, were used from 968 stations [73]. *GWT recorded during groundwater quality measurements* are recorded on-site during pumping. These data have high measurement errors <1 K due to exposure to surface condition, temperature changes caused during pumping, and differences in the sampling routine. Accuracy and precision of the used probes are below 0.2 K.

In this study we use the term aquifer temperature as a measure for the temperature at depths between 15 and 25 m bgl. This depth interval was cropped from temperature logs and available quality and logger data, because it is typically below the water table, within the vertical extent of the aquifer, and the depth in which historic temperature records are available [61, 62]. To resolve the aquifer temperature for each station, annual arithmetic means from the three data groups were calculated separately. Afterwards, the mean of these was calculated where applicable for each station, which resulted in 2999 annual mean values at 253 stations. Gaps in the annual mean values of the aquifer temperature were filled by linear interpolation within the data limits to achieve higher temporal coverage. Hereby, 1662 at 159 stations were filled. The total number of annual mean values for the aquifer is 4661 at 253 stations.

Groundwater data are analyzed on an annual basis in this study. However, seasonal variations at depths between 15 and 25 m bgl are above the typical temperature range in natural conditions that is below 0.1 K for depths below 15 m bgl. The mean seasonal temperature range observed at 57 stations in quarterly repeated temperature logs between September 2018 and 2019 is 0.5 K at 15 m bgl, 0.2 K at 20 m bgl, and 0.1 K at 30 m bgl. The year-to-year variability or annual reproducibility, expressed by the difference of the September temperature in 2019 and 2018 is around +0.1 K for the entire depth interval. Permanently installed loggers in the area indicate the same seasonal temperature range and year-to-year variability as the quarterly temperature logs.

### 2.3. TGP

The TGP defines the additional energy content in a reservoir towards natural conditions, without taking

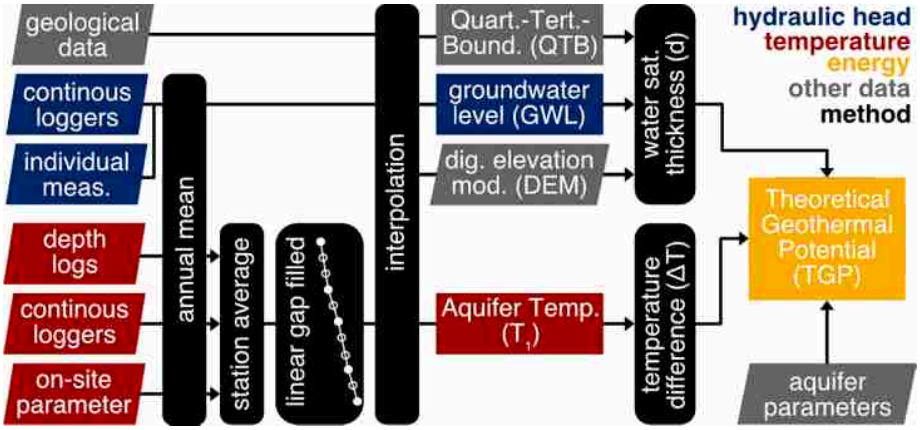


**Figure 2.** Methodology flowchart.

into account technical accessibility, economic feasibility and legislative regulations [6]. TGP can be calculated for water saturated porous aquifers by the equation [5, 6, 61]:

$$\mathrm{TGP} = ((1-n) \times c_w + n \times c_s) \times \Delta T \times A \times d,$$

where $n$ is the porosity, $c_w$ and $c_s$ are the volumetric heat capacities of the fluid (4.15 MJ $K^{-1}$ $m^{-3}$) and porous media (2.1 MJ $K^{-1}$ $m^{-3}$). $\Delta T$ (K) is the temperature difference ($\Delta T = T_1 - T_0$) between local aquifer temperature ($T_1$) and the proposed natural background temperature in 1973 of 10.8 °C ($T_0$). The TGP was calculated for a respective reservoir volume that was discretized by a 100 × 100 m grid ($A$) with variable saturated thickness ($d$). The saturated thickness ($d$ = min(min(GWL, DEM) − QTB), 0)) was calculated between the GWL, the DEM surface elevation, and the QTB (figure 2).

### 2.4. Spatial interpolation and time resolution

TGP, aquifer temperature and hydraulic heads were gathered as annual mean values and calculated for each year from 1973 to 2020. The QTB was assumed to be constant through time and calculated from all available data. All data is interpolated using standard inverse distance weighting on a 100 m × 100 m grid considering the nearest 15 data points and to a power of 1.5. Interpolated surfaces were smoothed by applying a Gaussian filter with two standard deviations.

### 2.5. Comparative data

To compare trends in GWT air temperature data were accessed from the Climate Data Center [76] of the German Meteorological Survey (DWD). Data was recorded hourly 2 m above ground, quality controlled, and resampled by the DWD. To relate the resolved TGP to regional residential space heating demand statistics for Germany [77] were projected to the city zones by the number of inhabitants in 2020 of the town quarters [78] and surrounding municipalities [79]. To reduce annual variations, the mean of the annual residential space heating demand between 2010 and 2020 was taken as a reference.

## 3. Results and discussion

### 3.1. Aquifer temperature

The GWT in the Cologne area is conditioned by a SUHI phenomenon with the temperature being highest underneath the city center and gradually decreasing towards the rural areas. The presented temperatures are monitored in the typical depth of the shallow aquifer between 15 and 25 m bgl. We refer to four zones of decreasing age and building density, from the city center, inner and outer city, to the outskirts. Figure 3 delineates the spatial distribution of the aquifer temperature beneath Cologne displayed as mean value of eight year periods since 1973. In every time period, temperature declines from the city center area towards the outskirts over the past 48 years. The temperature anomaly between the city center and the outskirts varies in time and rises by roughly 60% from +1.8 K in the 1973–1980 period to +2.9 K in the 2013–2020 period. Within the city zones temperature rise is highest in the city center at +2.0 K and significantly lower in the outer city and outskirts at below +1 K difference between the 2013–2020 and the 1973–1980 period (figure 3).

To better describe groundwater warming we performed regression analysis of the regional annual mean values of the aquifer in the four city zones, as well as in timeseries sensed at individual wells, and compared these to changes in ambient air temperature. The rate at which aquifer temperature is increasing is displayed versus the temperature in 2020 in figure 4. Assuming a linear behavior, the annual mean aquifer temperature in the city zones reveals a positive temperature shift of 0.52 ± 0.01, 0.29 ± 0.01, 0.22 ± 0.01, 0.24 ± 0.02 K $dec^{-1}$ for

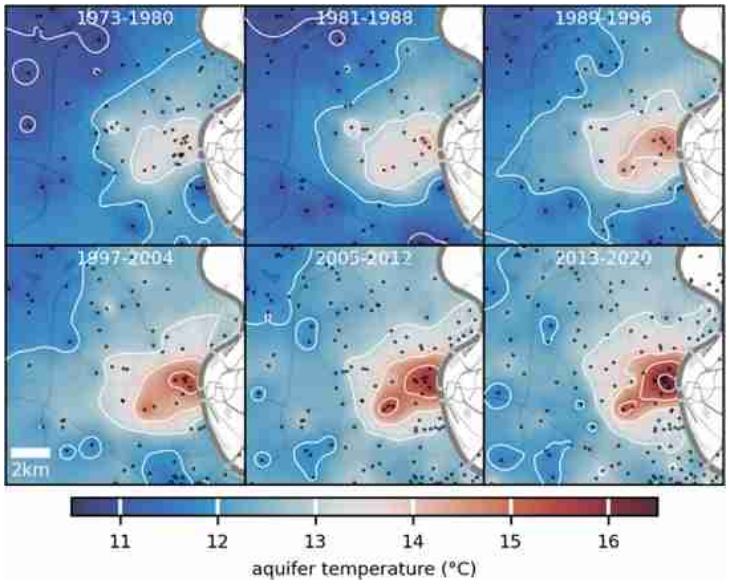


**Figure 3.** Mean aquifer temperature between 15 and 25 m bgl of eight year periods. Observation wells with data in the respective period are given as black dots. Regional extent is 13 km × 13 km.

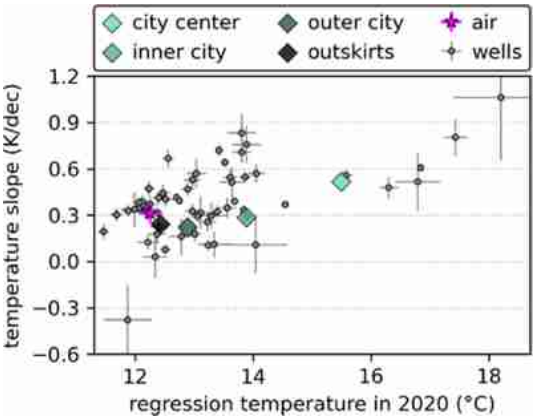


**Figure 4.** Temperature trends of 64 individual wells, regional mean in city zones, and 2 m air temperature. Error bars represent the standard errors of the linear regression.

the city center, inner and outer city and outskirts, respectively (figure 4). The annual means of the city zones indicate a strong correlation with time supported by squared Pearson correlation coefficients ranging between 0.97 and 0.84. The city zone values are supported by linear regression results of time series at individual wells, displayed in figure 4, that comprise at least 30 years and have a median slope of 0.37 K dec$^{-1}$. Three of 64 timeseries exceeded a mean squared error towards the regression line of 0.5 K. Two of them are the actual maximum and minimum slopes at 1.06 and −0.37 K dec$^{-1}$. Sixty-three out of the 64 wells indicate a positive temperature trend, and the one well that carries a negative trend is next to a flooded open pit mine with monitoring starting after reclamation in 1978. The maximum slope is observed directly in the city center and indicates a high rise in temperature with more than 20 °C measured in 2020 (15 °C–16 °C in 2009, and 17 °C–18 °C in 2018 and 2019).

Between 1973 and 2020, ambient annual air temperature means indicate a rise of 0.31 ± 0.06 K dec$^{-1}$ ($R^2 = 0.34$). Compared to aquifer temperature gradients in the rural parts (outskirts and outer city), the lapse rate in air temperature is about 25% higher. This trailing equals rates that are typically found when comparing temperature in air to the shallow subsurface [65, 80, 81]. The underground temperature gradient in the city center is contrarily exceeding atmospheric temperature rise and can be attributed to higher anthropogenic heat fluxes caused by a higher building density, surface imperviousness, and more underground buildings in this area [64]. Subsurface temperature shift in the inner city reflects a transition between the rural outskirts and the city center. It is assumed that the temperature rise in response to heated basements and surfaces is limited as the heat flux is effectively reduced when subsurface temperature is at the same level as the basement temperature. The strongest increase in temperature is observed between the 1980s and the middle of the 2000s, in which the rise in temperature is highest in all areas (cf table 1). Between the second (1981–1988) and fourth (1997–2004) period, temperature rise per period is highest at roughly +0.5 K in the city center and +0.3 K in the other city parts. In the past two periods (2005–2012 and 2013–2020) the temperature increase per period is reduced to +0.3 K in the city center and to around +0.1 K or below in the other city areas per period and in the same magnitude as between the first two periods (1973–1980 and 1981–1988).

**Table 1.** Mean aquifer temperature of eight year periods in the different city zones. Temperature is given in °C with the standard deviation in brackets (±1$\sigma$).

| City zone | 1973–1980 | 1981–1988 | 1989–1996 | 1997–2004 | 2005–2012 | 2013–2020 |
|---|---|---|---|---|---|---|
| City center | 13.2 (±0.5) | 13.5 (±0.5) | 14.1 (±0.5) | 14.6 (±0.6) | 14.9 (±0.6) | 15.2 (±0.8) |
| Inner city | 12.6 (±0.5) | 12.7 (±0.6) | 13.0 (±0.6) | 13.3 (±0.7) | 13.6 (±0.7) | 13.7 (±0.6) |
| Outer city | 12.0 (±0.5) | 12.0 (±0.5) | 12.3 (±0.4) | 12.6 (±0.4) | 12.7 (±0.3) | 12.7 (±0.3) |
| Outskirts | 11.4 (±0.4) | 11.4 (±0.3) | 11.8 (±0.4) | 12.1 (±0.4) | 12.2 (±0.3) | 12.3 (±0.3) |
| Total | 11.8 (±0.6) | 11.9 (±0.7) | 12.2 (±0.7) | 12.5 (±0.7) | 12.6 (±0.7) | 12.7 (±0.8) |

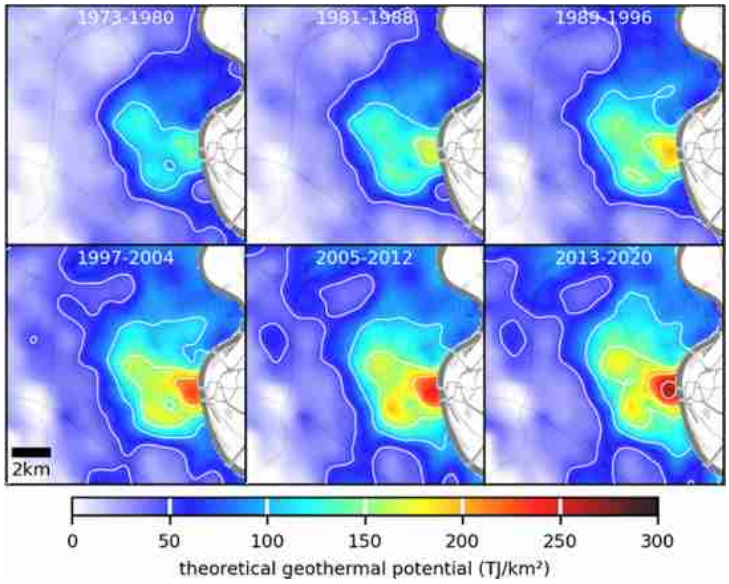


**Figure 5.** Theoretical geothermal potential of eight year periods. Regional extent is 13 km × 13 km.

### 3.2. TGP of shallow urban groundwater

We quantified the TGP of the urban aquifer based on the vertical extent of the aquifer, the water saturated thickness, and the aquifer temperature. The TGP mirrors the trends seen in aquifer temperature and is highest in the city center area in all periods, while increasing over time as illustrated in figure 5. In all city zones, TGP exhibits a strictly increasing trend over time with mean values (±1 std. dev.) of 117, 83, 49, and 18 TJ km$^{-2}$ in the 1973–80 period and 202, 130, 79, and 43 TJ km$^{-2}$ in the 2013–20 period in the city center, inner city, outer city and outskirts, respectively. In the SW of the study area the TGP is zero, because the Quaternary terrace deposits that host the aquifer wedge out in this region.

While the TGP density is highest in the central parts, the total energy content is actually lowest in the city center at 936 TJ, due to the small fraction of the city area (cf table 2). Compared to the estimated residential heating demand for this area, the city center yields the highest capacity for supplying residential space heating. The additional energy stored in the city center in the 2013–20 period would equal the demand of about 1 year. In the surrounding city zones this ratio is slightly lower, equaling between 79% and 95% of the annual residential heating demand.

However, this stationary calculation of the TGP as a one-time extractable heat reservoir formed by anthropogenic heating on top of the potential of natural conditions and neglects transient effects and technical accessibility of the energy. To resolve the energy that is constantly stored in the aquifer we performed a linear regression of the annual area means of the four city zones (figure 6). The regression yields a storage rate of 27 mW m$^{-2}$ for the total area, and 70, 39, 26, 22 mW m$^{-2}$ for the respective city zones (table 2). Even though heat storage is three magnitudes higher in the city center when compared to the outskirts, the heat stored in the aquifer each year equals only 1% of the thermal demand. These storage rates are also significantly lower than the average anthropogenic heat flux of 390 mW m$^{-2}$ from the surface towards the aquifer that was calculated by Benz *et al* [64] using a 1D analytical model for this area. This implies that only about 5%–20% of the energy that is released into urban underground is also stored within the aquifer in the form of heat. The calculated shares of the TGP reflect the observed energy growth of the aquifers thermal reservoir in time and are related to an average thermal demand, which either over- or underestimates the potential, as heating loads in Germany have an annual variation

**Table 2.** Mean aquifer temperature, theoretical geothermal potential (TGP), and water saturated thickness (SAT) of eight year periods in the different city zones. Groundwater temperature (GWT) is given in °C with the standard deviation in brackets ($\pm 1\sigma$).

| City zone | Population | Area | Residential space heating demand | | TGP (2013–20) | | TGP cap. | TGP shift | GWT shift | Median GWT 2013–20 | Mean SAT |
|---|---|---|---|---|---|---|---|---|---|---|---|
| Unit | k | $km^2$ | $TJ\ yr^{-1}$ | $W\ m^{-2}$ | TJ | $TJ\ km^{-2}$ | yr | $mW\ m^{-2}$ | $K\ dec^{-1}$ | °C | M |
| City center | 45 | 4.6 | 927 | 6.39 | 936 | 202 | 1.0 | $70.2 \pm 2.4$ | $0.52 \pm 0.01$ | 15.3 | 17.6 |
| Inner city | 180 | 22.3 | 3683 | 5.24 | 2897 | 130 | 0.8 | $39.4 \pm 1.8$ | $0.29 \pm 0.01$ | 13.6 | 16.3 |
| Outer city | 185 | 45.1 | 3780 | 2.66 | 3575 | 79 | 1.0 | $25.7 \pm 1.6$ | $0.22 \pm 0.01$ | 12.7 | 13.7 |
| Outskirts | 190 | 78.1 | 3896 | 1.58 | 3332 | 43 | 0.9 | $21.6 \pm 1.0$ | $0.24 \pm 0.02$ | 12.2 | 9.4 |
| Total area | 600 | 150.1 | 12 285 | 2.60 | 10 739 | 72 | 0.9 | $26.9 \pm 1.2$ | $0.25 \pm 0.01$ | 12.5 | 12.0 |
| City area | 410 | 72.0 | 8389 | 3.69 | 7407 | 103 | 0.9 | $32.8 \pm 1.6$ | $0.26 \pm 0.01$ | 12.9 | 14.8 |

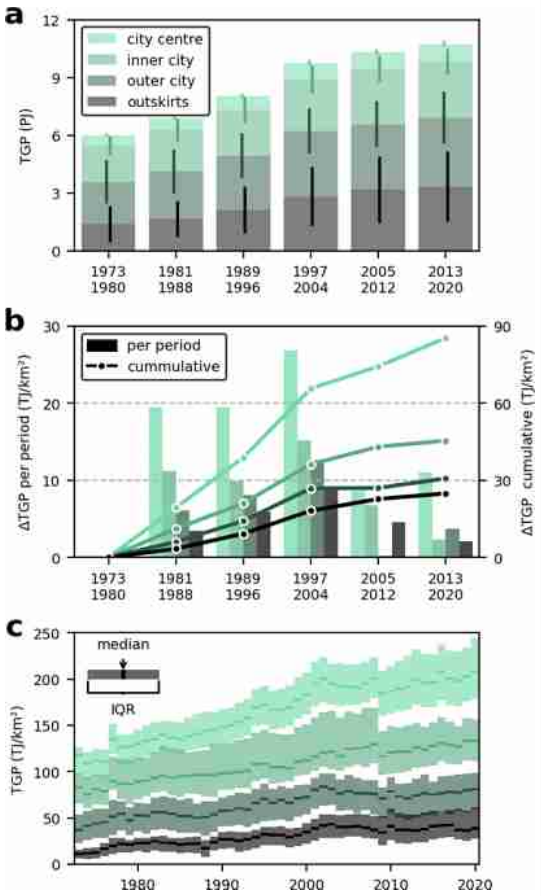


**Figure 6.** (a) Total theoretical geothermal potential (TGP) of city zones for eight year periods. Error lines indicate standard deviation in zonal distributions. (b) Cumulative and absolute TGP change per period. (c) Interquartile range (IQR) and median TGP per area for city zones.

of around ±10%. In addition, the actual operative potential for shallow geothermal systems will be much higher if we consider mixed heating and cooling applications, transient heat transport, and if a depletion of the of the thermal reservoir is allowed. The thermal conditions in the aquifer tend to equilibrate from the year 2000 and onwards (figure 6(b)) and the net heat gain thus declines over time. However, recharge of the shallow ground would dynamically adapt if more energy would be extracted. In order to describe dynamic phenomenons such as groundwater flow, heat loss towards the aquifer boundaries, or changes caused by shallow geothermal systems under specific thermal loads, a numerical model would be needed which is beyond the scope of this study.

The gross energy which is not stored in the aquifer is transported by groundwater advection outside its vertical or lateral extent. Vertical conductive heat transport towards greater depths in this area is less efficient than lateral advective heat transport by groundwater flow, that is oriented in north-eastern direction towards the receiving stream. Numerical model results of this area suggest that the annual heat loss towards the river is around 610 TJ per year [66], that equals 5% of the total TGP. In vertical direction the shallow aquifer is typically at depths between 10 to 30 m bgl. In this zone, shallow geothermal energy can be effectively harnessed by especially open-loop groundwater heat pump systems. Anthropogenic heat is also stored in the underlying aquitard down to a depth of at least 100 m bgl as is evident from borehole temperature logs and model results [66]. Similar penetration depths between 60 and 130 m bgl are reported for other cities [46, 51, 82]. The energy stored in the underlying aquitard could also be accessed using for example borehole heat exchangers in combination with ground source heat pump systems. In addition, the UHI phenomenon affects the unsaturated zone. Analytical simulation shows that under natural and urban green surfaces the heat flux can be reversed and cool the urban subsurface [64, 83]. Natural surfaces also have major cooling effects on atmospheric UHIs [84].

To quantify heat losses and heat fluxes inside and outside the aquifer spatially and temporally, detailed numerical models can be used. Models of comparable urban aquifers containing river boundaries [23, 57, 85] revealed that rivers can have a significant effect on the thermal state of urban aquifers by infiltration and exfiltration in the river beds and by flooding events. Such models can also be employed to balance heat fluxes based on implemented surface boundary conditions. Recent modeling results for Cardiff (UK) suggest surface averaged heat fluxes at a rate of 60 mW $m^{-2}$ at 20 m bgl [86].

### 3.3. Further implications

Urban subsurface is characterized by temperatures that are anthropogenically altered by continuous heat release over large areas and long periods. The opportunity to extract the accumulated heat is often overlooked, and together with the naturally stored heat, shallow geothermal energy will gain importance for integrated heat supply in cities. Clearly, as demonstrated for the city of Cologne, SUHIs tend to reach a quasi-steady thermal condition that follows atmospheric warming, and the urban heat in place as expressed by the TGP thus will not substantially increase more than elsewhere in the future. However, the geothermal usage potential can substantially be enhanced by active urban-scale subsurface heat extraction, which accelerates the ground heat gain and thus stimulates large-scale urban heat recycling. This means, by concerted application of great numbers of ground source and groundwater heat pump systems [14, 15, 49], the urban underground will absorb more energy while losing less heat *in-situ* by lateral groundwater flow and exfiltration to rivers. Such active subsurface temperature regulation will not only be beneficial for heat supply, but is essential for facilitating effective cooling by utilization of groundwater. This bivalent use of aquifers as heat source and sink is the ideal solution, especially considering that in many cities the thermal stress

for shallow aquifers is augmented by residential and industrial cooling demands [87]. The relative importance of cooling will increase in the future with global warming and improved insulation of buildings.

Active control and regulation of further heat accumulation is necessary not only for optimizing urban subsurface geothermal use. Warming of aquifers deteriorates groundwater quality by oxygen depletion and enhanced mobilization of contaminants. Warmed groundwater stimulates growth of pathogenic microbes while modifying biodiversity and character of groundwater ecosystems [88, 89]. For buried structures, there is a need for thermal insulation, and especially the temperature of drinking water is reported to rise in cities due to warming of the buried supply network [90].

## 4. Conclusions

Based on five decades of monitoring for the city of Cologne, we found that the shallow aquifer temperature is rising continuously. In the city center, where urbanization is most dense, temperature rise is highest at a rate of 0.52 K $dec^{-1}$. This decreases towards the outer city and outskirts where it is less than half as high at rates of 0.22 and 0.24 K $dec^{-1}$. Compared to the rise in ambient surface temperature of 0.31 K $dec^{-1}$, rates in the shallow subsurface of the less densely populated areas indicate the expected trailing response to atmospheric climate variations, while in the city center subsurface warming is increased compared to surface warming. A SUHI is present since the start of recordings but is rising in intensity over time. In the 1970s aquifer temperature in the city center was elevated by +1.8 K on average towards the rural area. This temperature anomaly expanded by about 60% to +2.9 K in recent years. It is expected that the SUHI phenomenon will continue as a response to atmospheric warming. However, we see a reduction of the rate at which urban subsurface is heated in the past two decades. This suggests that the aquifer is approaching a temperature level at which the steady temperature from buried infrastructure and basements result in reduced thermal gradients and equilibrated heat fluxes.

The elevated temperature translates to additional heat that is stored in the aquifer. Compared to natural conditions in the 1970s, the additional heat stored in the aquifer domain equals the city's residential heating demand of around one year. However, the rate at which energy accumulates is relatively low and equals only about 1% of the residential heating demand. Compared to calculations of the anthropogenic heat flux into the urban subsurface, the rate at which energy is stored in the aquifer domain over time is one magnitude lower. The low storage ratio of the emitted waste heat is attributed to both lateral heat transport towards the adjacent river and vertical surpassing of the depths of the aquifer. This implies that on the one hand, the capacity of using only the aquifer for sustainable space heating is not promising, and that on the other hand, the heat reaching the groundwater is to a large proportion trespassing the thin aquifer layer and not stored over time.

However, the potential for modern shallow geothermal units that combine heating and cooling is not based on depletion of a thermal reservoir. Sustainable operation of such aquifer thermal energy storage systems relies heavily on balancing heating and cooling loads and achieving constant year-to-year temperature in the reservoir. For these systems, the SUHI phenomenon acts as a regional imbalance and is a major factor to be considered to achieve longevity and sustainability. Especially cooling applications suffer from higher ground temperature but see a rising demand in response to climate, technological and socio-economical change. The observed trend in reduction of the heat accumulation in recent times could be crucial for the availability of urban underground as a promising resource for cooling applications, and a key component in the transition towards renewables.

## Data availability statement

The data that support the findings of this study are available upon request from the authors.

## Acknowledgments

We thank Leonhard Zimmerer, Rafael Meinhardt, Johannes Granzow and Christoph Bott for their great support during the field measurements. We also thank the Erftverband, the Rheinenergie, and the municipality of the city of Cologne for providing groundwater data and access to the monitoring wells. This work is funded by the German Research Foundation, DFG (Grant No. BA2850/3-1).

## ORCID iDs

Hannes Hemmerle https://orcid.org/0000-0001-7510-6633
Grant Ferguson https://orcid.org/0000-0001-8519-1771
Philipp Blum https://orcid.org/0000-0001-7418-0954
Peter Bayer https://orcid.org/0000-0003-4884-5873

## References

[1] Oke T R 1982 The energetic basis of the urban heat island *Q. J. R. Meteorol. Soc.* **108** 1–24
[2] Ferguson G and Woodbury A D 2007 Urban heat island in the subsurface *Geophys. Res. Lett.* **34** L23713
[3] Hsu A, Sheriff G, Chakraborty T and Manya D 2021 Disproportionate exposure to urban heat island intensity across major US cities *Nat. Commun.* **12** 2721

[4] Lo Y T E et al 2019 Increasing mitigation ambition to meet the Paris Agreement's temperature goal avoids substantial heat-related mortality in U.S. cities Sci. Adv. 5 eaau4373
[5] Zhu K, Blum P, Ferguson G, Balke K-D and Bayer P 2010 The geothermal potential of urban heat islands Environ. Res. Lett. 5 044002
[6] Bayer P, Attard G, Blum P and Menberg K 2019 The geothermal potential of cities Renew. Sustain. Energy Rev. 106 17–30
[7] IEA 2018 The Future of Cooling (Paris: IEA)
[8] Yalew S G et al 2020 Impacts of climate change on energy systems in global and regional scenarios Nat. Energy 5 794–802
[9] van Ruijven B J, De Cian E and Wing I S 2019 Amplification of future energy demand growth due to climate change Nat. Commun. 10 1–12
[10] Department of Economic and PD Social Affairs, United Nations 2018 World Urbanization Prospects: The 2018 Revision online edn (New York: Department of Economic and Social Affairs PD)
[11] Ritchie H and Roser M 2018 Urbanization (Our World in Data)
[12] Kammen D M and Sunter D A 2016 City-integrated renewable energy for urban sustainability Science 352 922–8
[13] Henry A, Prasher R and Majumdar A 2020 Five thermal energy grand challenges for decarbonization Nat. Energy 5 635–7
[14] Couderc E 2017 Geothermal energy: underground urban scene Nat. Energy 2 16212
[15] Rivera J A, Blum P and Bayer P 2017 Increased ground temperatures in urban areas: estimation of the technical geothermal potential Renew. Energy 103 388–400
[16] Arola T and Korkka-Niemi K 2014 The effect of urban heat islands on geothermal potential: examples from quaternary aquifers in Finland Hydrogeol. J. 22 1953–67
[17] Allen A, Milenic D and Sikora P 2003 Shallow gravel aquifers and the urban 'heat island' effect: a source of low enthalpy geothermal energy Geothermics 32 569–78
[18] Bucci A, Barbero D, Lasagna M, Forno M G and De Luca D A 2017 Shallow groundwater temperature in the Turin area (NW Italy): vertical distribution and anthropogenic effects Environ. Earth Sci. 76 221
[19] Buday T et al 2019 Subsurface urban heat island investigation in Debrecen, Hungary based on archive and recently measured data European Geothermal Congress 2019 (Den Haag, The Netherlands, 11-14 June 2019)
[20] Changnon S A 1999 A rare long record of deep soil temperatures defines temporal temperature changes and an urban heat island Clim. Change 42 531–8
[21] Djebebe-Ndjiguim C L, Huneau F, Denis A, Foto E, Moloto-a-kenguemba G, Celle-Jeanton H, Garel E, Jaunat J, Mabingui J and Le Coustumer P 2013 Characterization of the aquifers of the Bangui urban area, Central African Republic, as an alternative drinking water supply resource Hydrol. Sci. J. 58 1760–78
[22] Eggleston J and McCoy K J 2015 Assessing the magnitude and timing of anthropogenic warming of a shallow aquifer: example from Virginia Beach, USA Hydrogeol. J. 23 105–20
[23] Epting J, García-Gil A, Huggenberger P, Vázquez-Suñe E and Mueller M H 2017 Development of concepts for the management of thermal resources in urban areas–assessment of transferability from the Basel (Switzerland) and Zaragoza (Spain) case studies J. Hydrol. 548 697–715
[24] Farr G, Patton A M, Boon D P, James D R, Williams B and Schofield D I 2017 Mapping shallow urban groundwater temperatures, a case study from Cardiff, UK Q. J. Eng. Geol. Hydrogeol. 50 187–98
[25] Ford M and Tellam J 1994 Source, type and extent of inorganic contamination within the Birmingham urban aquifer system, UK J. Hydrol. 156 101–35
[26] García-Gil A, Epting J, Garrido E, Vázquez-Suñé E, Lázaro J M, Sánchez Navarro J Á, Huggenberger P and Calvo M Á M 2016 A city scale study on the effects of intensive groundwater heat pump systems on heavy metal contents in groundwater Sci. Total Environ. 572 1047–58
[27] Headon J, Banks D, Waters A and Robinson V K 2009 Regional distribution of ground temperature in the Chalk aquifer of London, UK Q. J. Eng. Geol. Hydrogeol. 42 313–23
[28] Hemmerle H, Hale S, Dressel I, Benz S A, Attard G, Blum P and Bayer P 2019 Estimation of groundwater temperatures in Paris, France Geofluids 2019 1–11
[29] Huang F, Zhan W, Wang Z-H, Voogt J, Hu L, Quan J, Liu C, Zhang N and Lai J 2020 Satellite identification of atmospheric-surface-subsurface urban heat islands under clear sky Remote Sens. Environ. 250 112039
[30] Kazemi G A 2011 Impacts of urbanization on the groundwater resources in Shahrood, Northeastern Iran: comparison with other Iranian and Asian cities Phys. Chem. Earth A/B/C 36 150–9
[31] Klene A, Hinkel K and Nelson F 2003 The barrow urban heat island study: soil temperatures and active-layer thickness Proc. 8th Int. Conf. on Permafrost (Lisse: AA Balkema)
[32] Lee J-Y and Han J 2013 Evaluation of groundwater monitoring data in four megacities of Korea: implication for sustainable use Nat. Resour. Res. 22 103–21
[33] Lokoshchenko M and Korneva I 2015 Underground urban heat island below Moscow city Urban Clim. 13 1–13
[34] Marschalko M, Krčmář D, Yilmaz I, Fľaková R and Ženišová Z 2018 Heat contamination in groundwater sourced from heat pump for heating in Bratislava (Slovakia)'s historic centre Environ. Earth Sci. 77 1–12
[35] Menberg K, Bayer P, Zosseder K, Rumohr S and Blum P 2013 Subsurface urban heat islands in German cities Sci. Total Environ. 442 123–33
[36] Morris B L, George Darling W, Gooddy D C, Litvak R G, Neumann I, Nemaltseva E J and Poddubnaia I 2006 Assessing the extent of induced leakage to an urban aquifer using environmental tracers: an example from Bishkek, capital of Kyrgyzstan, Central Asia Hydrogeol. J. 14 225–43
[37] Mount H and Hernandez L 2002 Soil temperatures and anthropogenic soils ICOMANTH Report ed J M Galbraith,H R Mount and J M Scheye No. 1. CD-ROM (Lincoln, NE: USDA-NRCS) pp 22-1–22-9
[38] Müller N, Kuttler W and Barlag A-B 2014 Analysis of the subsurface urban heat island in Oberhausen, Germany Clim. Res. 58 247–56
[39] Öngen A S, Öngen A S and Ergüler Z A 2021 The effect of urban heat island on groundwater located in shallow aquifers of Kutahya city center and shallow geothermal energy potential of the region Bull. Miner. Res. Explor. 165 217–34
[40] Previati A and Crosta G B 2021 Characterization of the subsurface urban heat island and its sources in the Milan city area, Italy Hydrogeol. J. 29 1–14
[41] Salem Z, Sakura Y and Aslam M M 2004 The use of temperature, stable isotopes and water quality to determine the pattern and spatial extent of groundwater flow: Nagaoka area, Japan Hydrogeol. J. 12 563–75
[42] Savva Y, Szlavecz K, Pouyat R V, Groffman P M and Heisler G 2010 Effects of land use and vegetation cover on soil temperature in an urban ecosystem Soil Sci. Soc. Am. J. 74 469–80
[43] Schweighofer J A, Wehrl M, Baumgärtel S and Rohn J 2021 Detecting groundwater temperature shifts of a subsurface urban heat island in SE Germany Water 13 1417
[44] Schweighofer J A, Wehrl M, Baumgärtel S and Rohn J 2021 Calculating energy and its spatial distribution for a subsurface urban heat island using a GIS-approach Geosciences 11 24
[45] Tang C-S, Shi B, Gao L, Daniels J L, Jiang H-T and Liu C 2011 Urbanization effect on soil temperature in Nanjing, China Energy Build. 43 3090–8
[46] Taniguchi M, Uemura T and Sakura Y 2005 Effects of urbanization and groundwater flow on subsurface

temperature in three megacities in Japan *J. Geophys. Eng.* **2** 320–5
[47] Taniguchi M, Uemura T and Jago-on K 2007 Combined effects of urbanization and global warming on subsurface temperature in four Asian cities *Vadose Zone J.* **6** 591–6
[48] Taylor C A and Stefan H G 2009 Shallow groundwater temperature response to climate change and urbanization *J. Hydrol.* **375** 601–12
[49] Tissen C, Menberg K, Benz S A, Bayer P, Steiner C, Götzl G and Blum P 2021 Identifying key locations for shallow geothermal use in Vienna *Renew. Energy* **167** 1–19
[50] Turkoglu N 2010 Analysis of urban effects on soil temperature in Ankara *Environ. Monit. Assess.* **169** 439–50
[51] Visser P W, Kooi H, Bense V and Boerma E 2020 Impacts of progressive urban expansion on subsurface temperatures in the city of Amsterdam (The Netherlands) *Hydrogeol. J.* **28** 1755–72
[52] Vranjes A, Milenic D and Dokmanovic P 2015 Geothermal concept for energy efficient improvement of space heating and cooling in highly urbanized area *Therm. Sci.* **19** 857–64
[53] Westaway R and Younger P L 2016 Unravelling the relative contributions of climate change and ground disturbance to subsurface temperature perturbations: case studies from Tyneside, UK *Geothermics* **64** 490–515
[54] Yalcin T and Yetemen O 2009 Local warming of groundwaters caused by the urban heat island effect in Istanbul, Turkey *Hydrogeol. J.* **17** 1247–55
[55] Yamano M, Goto S, Miyakoshi A, Hamamoto H, Lubis R F, Monyrath V and Taniguchi M 2009 Reconstruction of the thermal environment evolution in urban areas from underground temperature distribution *Sci. Total Environ.* **407** 3120–8
[56] Yusuf K 2007 Evaluation of groundwater quality characteristics in Lagos-City *J. Appl. Sci.* **7** 1780–4
[57] Attard G, Rossier Y, Winiarski T and Eisenlohr L 2016 Deterministic modeling of the impact of underground structures on urban groundwater temperature *Sci. Total Environ.* **572** 986–94
[58] Bidarmaghz A, Choudhary R, Soga K, Kessler H, Terrington R L and Thorpe S 2019 Influence of geology and hydrogeology on heat rejection from residential basements in urban areas *Tunn. Undergr. Space Technol.* **92** 103068
[59] Epting J, Händel F and Huggenberger P 2013 Thermal management of an unconsolidated shallow urban groundwater body *Hydrol. Earth Syst. Sci.* **17** 1851–69
[60] Bayer P, Rivera J A, Schweizer D, Schärli U, Blum P and Rybach L 2016 Extracting past atmospheric warming and urban heating effects from borehole temperature profiles *Geothermics* **64** 289–99
[61] Balke K 1974 The thermal impact of populated areas on groundwater, illustrated by the example of the city of Cologne (Der thermische Einfluss besiedelter Gebiete auf das Grundwasser, dargestellt am Beispiel der Stadt Köln) *GWF-Wasser/Abwasser* **115** 117–24
[62] Balke K-D and Kley W 1981 Groundwater temperatures in metropolitan areas (Die Grundwassertemperaturen in Ballungsgebieten) *Bundesministerium für Forschung und Technologie—Forschungsbericht* **T 81-028** 91
[63] Balke K 1977 Groundwater as a source of energy (Das Grundwasser als Energieträger) *Brennst.-Wärme-Kraft* **29** 191–94
[64] Benz S A, Bayer P, Menberg K, Jung S and Blum P 2015 Spatial resolution of anthropogenic heat fluxes into urban aquifers *Sci. Total Environ.* **524** 427–39
[65] Menberg K, Blum P, Kurylyk B L and Bayer P 2014 Observed groundwater temperature response to recent climate change *Hydrol. Earth Syst. Sci.* **18** 4453–66
[66] Zhu K, Bayer P, Grathwohl P and Blum P 2015 Groundwater temperature evolution in the subsurface urban heat island of Cologne, Germany *Hydrol. Process.* **29** 965–78
[67] Benz S A, Bayer P, Goettsche F M, Olesen F S and Blum P 2016 Linking surface urban heat islands with groundwater temperatures *Environ. Sci. Technol.* **50** 70–78
[68] Meng B, Vienken T, Kolditz O and Shao H 2019 Evaluating the thermal impacts and sustainability of intensive shallow geothermal utilization on a neighborhood scale: lessons learned from a case study *Energy Convers. Manage.* **199** 111913
[69] Vienken T, Kreck M and Dietrich P 2019 Monitoring the impact of intensive shallow geothermal energy use on groundwater temperatures in a residential neighborhood *Geotherm. Energy* **7** 1–14
[70] Balke K-D 1973 Geothermische und hydrogeologische Untersuchungen in der südlichen Niederrheinischen Bucht *Geologisches Jahrbuch* vol C 5, ed H Karrenberg (Stuttgart: Schweizerbart Science Publishers) p 61 (available at: www.schweizerbart.de//publications/detail/isbn/9783510962518/Geologisches_Jahrbuch_Reihe_C_Heft)
[71] Hilden H 1988 Geology of the lower Rhine (Geologie am Niederrhein) (Geologisches Landesamt Nordrhein-Westfalen, Krefeld) p 142
[72] Klostermann J 1992 The quaternary of the lower Rhenish Bight (Das Quartär der Niederrheinischen Bucht) (Geologisches Landesamt Nordrhein-Westfalen, Krefeld) p 200
[73] ELWAS 2013 Electronic water management network for water management authorities in North Rhine-Westphalia (available at: www.elwasweb.nrw.de) (Accessed 21 March 2021)
[74] DABO 2020 Borehole Database (Bohrungsdatenbank DABO) maintained by the Geological Survey of North Rhine-Westphalia (GD NRW) (available at: www.bohrungen.nrw.de) (Accessed 1 April 2021)
[75] OpenGeoDataNRW 2021 Digital elevation model—grid width 1m. State of North Rhine-Westphalia, Cologne District Government, Geobasis NRW (available at: www.opengeodata.nrw.de) (Accessed 1 April 2021)
[76] CDC 2021 Climate data center (CDC) (available at: opendata.dwd.de) (Accessed 21 March 2021)
[77] BMWi 2020 Energy efficiency in figures—developments and trends in Germany 2020 (Energieeffizienz in Zahlen—Entwicklungen und Trends in Deutschland 2020) B.f.W.u.E. (BMWi), Editor, Bundesministerium für Wirtschaft und Energie (BMWi) p 102
[78] StadtKöln 2021 Cologne district information population 2020 (Kölner Stadtteilinformationen Bevölkerung 2020) (available at: www.stadt-koeln.de) (Accessed 20 July 2021)
[79] IT.NRW 2021 Statistics and IT services: population in North Rhine-Westphalia (Statistik und IT-Dienstleistungen: bevölkerung in Nordrhein-Westfalen) (available at: www.it.nrw) (Accessed 21 April 2021)
[80] Hemmerle H and Bayer P 2020 Climate change yields groundwater warming in Bavaria, Germany *Front. Earth Sci.* **8** 575894
[81] Benz S A, Bayer P, Winkler G and Blum P 2018 Recent trends of groundwater temperatures in Austria *Hydrol. Earth Syst. Sci.* **22** 3143–54
[82] Ferguson G and Woodbury A D 2004 Subsurface heat flow in an urban environment *J. Geophys. Res.* **109** B02402
[83] Benz S A, Bayer P, Blum P, Hamamoto H, Arimoto H and Taniguchi M 2018 Comparing anthropogenic heat input and heat accumulation in the subsurface of Osaka, Japan *Sci. Total Environ.* **643** 1127–36
[84] Aram F, Higueras García E, Solgi E and Mansournia S 2019 Urban green space cooling effect in cities *Heliyon* **5** e01339
[85] García-Gil A, Vázquez-Suñe E, Schneider E G, Sánchez-Navarro J Á and Mateo-Lázaro J 2014 The thermal consequences of river-level variations in an urban groundwater body highly affected by groundwater heat pumps *Sci. Total Environ.* **485** 575–87

[86] Makasis N, Kreitmair M J, Bidarmaghz A, Farr G J, Scheidegger J M and Choudhary R 2021 Impact of simplifications on numerical modelling of the shallow subsurface at city-scale and implications for shallow geothermal potential *Sci. Total Environ.* **791** 148236
[87] Epting J, Müller M H, Genske D and Huggenberger P 2018 Relating groundwater heat-potential to city-scale heat-demand: a theoretical consideration for urban groundwater resource management *Appl. Energy* **228** 1499–505
[88] Blum P, Menberg K, Koch F, Benz S A, Tissen C, Hemmerle H and Bayer P 2021 Is thermal use of groundwater a pollution? *J. Contam. Hydrol.* **239** 103791
[89] Brielmann H, Griebler C, Schmidt S I, Michel R and Lueders T 2009 Effects of thermal energy discharge on shallow groundwater ecosystems *FEMS Microbiol. Ecol.* **68** 273–86
[90] Agudelo-Vera C *et al* 2020 Drinking water temperature around the globe: understanding, policies, challenges and opportunities *Water* **12** 1049